The Journal of Physical Chemistry A

 VOLUME 102, NUMBER 5, JANUARY 29, 1998

FEATURE ARTICLE

# "Direct" and "Correct" Calculation of Canonical and Microcanonical Rate Constants for Chemical Reactions

**William H. Miller**

*Department of Chemistry, University of California, and Chemical Sciences Division, Lawrence Berkeley Laboratory, Berkeley, California 94720*

*Received: October 2, 1997; In Final Form: November 24, 1997*

Theoretical approaches for calculating rate constants of chemical reactions—either the microcanonical rate for a given total energy $k(E)$ or the canonical rate for a given temperature $k(T)$—are described that are both "direct", i.e., bypass the necessity of having to solve the complete state-to-state quantum reactive scattering problem, yet also "correct", i.e., in principle exact (given a potential energy surface, assuming nonrelativistic quantum mechanics, etc.) Applications to a variety of reactions are presented to illustrate the methodology for various dynamical situations, e.g., transition-state-theory-like dynamics where the system moves directly through the interaction (transition-state) region and reactions that form long-lived collision complexes. It is also shown how this rigorous quantum theory can be combined with the Lindemann mechanism for describing the effects of collisions with a bath gas, so as to be able to treat recombination reactions and other effects of pressure. Finally, several ways are discussed for combining these rigorous approaches for small molecule dynamics with an approximate treatment of (perhaps many) other degrees of freedom (i.e., a solvent, a substrate, a cluster environment) that may be coupled to it.

## I. Introduction

If one wishes to describe a bimolecular chemical reaction at the most detailed level possible, i.e., its state-to-state differential scattering cross section, then it is necessary to solve the Schrödinger equation (with scattering boundary conditions) to obtain the **S**-matrix $\{S_{n_p,n_r}(E,J)\}$ as a function of total energy $E$ and total angular momentum $J$, in terms of which the cross sections can be calculated as follows:[1]

$$\sigma_{n_p \leftarrow n_r}(\theta,E) = |(2ik_{n_r})^{-1}\sum_J (2J+1)\, d^J_{m_p,m_r}(\theta)\, S_{n_p,n_r}(E,J)|^2 \quad (1.1)$$

Here $n_r$ ($n_p$) labels the reactant (product) rotational and vibrational states, $\theta$ is the scattering angle between the relative velocity vectors of reactants and products, $m_r$ ($m_p$) is the projection of total angular momentum onto the relative velocity vector of the reactants (products), and $d^J_{mm'}(\theta)$ is the Wigner rotation matrix. A number of such state-to-state quantum reactive scattering calculations have actually been carried out for simple reactions, mostly using time-independent scattering methodology based on the **S**-matrix Kohn variational approach[2] or coupled channel methods utilizing hyperspherical coordinates;[3] these include H or D + $H_2$(para) → $H_2$(ortho) or HD + H, F + $H_2$ → HF + H, Cl + $H_2$ → HCl + H, O + HCl → OH + Cl, O + $H_2$ → OH + H, and H + $O_2$ → OH + O.

In the vast majority of chemical applications, however, one needs only the *rate constant* for the reaction, either canonical (i.e, characterized by a temperature $T$), $k(T)$, or microcanonical (characterized by the total energy $E$), $k(E)$; $k(T)$ is usually the quantity of interest for bimolecular reactions, and $k(E)$ for unimolecular reactions. These rate constants are appropriate

S1089-5639(97)03208-8 CCC: $15.00 
Published on Web 01/14/1998

averages of the above cross sections and thus are readily available if a complete scattering calculation has been carried out to obtain the **S**-matrix. The result of this averaging process is contained very simply in the *cumulative reaction probability* (CRP) $N(E)$, which is defined as[4]

$$N(E) = \sum_J (2J+1) \sum_{n_p, n_r} |S_{n_p, n_r}(E,J)|^2 \tag{1.2}$$

and in terms of which the microcanonical and canonical rate constants $k(E)$ and $k(T)$ are given by

$$k(E) = [2\pi\hbar\rho_r(E)]^{-1} N(E) \tag{1.3a}$$

$$k(T) = [2\pi\hbar Q_r(T)]^{-1} \int_{-\infty}^{\infty} \mathrm{d}E\, \mathrm{e}^{-\beta E} N(E) \tag{1.3b}$$

where $\beta = (kT)^{-1}$, $\rho_r$ is the density of reactant states per unit energy, and $Q_r$ is the reactant partition function per unit volume.

The situation, therefore, is that if one has carried out a complete reactive scattering calculation and obtained the **S**-matrix, then everything about the reaction (in field-free space) is available, from the most detailed state-specific cross sections via eq 1.1 to the most averaged quantities, the rate constants via eqs 1.2 and 1.3 (or anything in between). However, if it is only the rate constants that are desired, then it clearly seems inefficient to have to obtain the complete **S**-matrix, with all its state-to-state information, and then average this out in constructing the CRP via eq 1.2. One thus seeks a *direct* way of calculating $N(E)$ (or $k(T)$ itself), i.e., one that avoids having to obtain the **S**-matrix, yet one that is also *correct*, i.e., without any inherent approximations. In applications to complex chemical reactions it will of course often be necessary to make approximations, but one would at least like to begin with a formulation that is free of them. To the extent that such an approach is possible, it is also reasonable to expect that one will be able to apply it to more complex reactions than those for which a complete reactive scattering calculation can be carried out, simply because one is seeking less detailed information about the reaction dynamics.

The purpose of this paper is to survey the methodology and recent applications of this "direct" and "correct" way of calculating reaction rate constants.[5] My own work in this general area began[6] in trying to formulate a more rigorous quantum mechanical version of transition-state theory (TST).[7] This was motivated by insightful work of Pechukas and McLafferty[8] which showed that, within the realm of classical mechanics, TST is actually an exact theory at sufficiently low energy. Low energy, of course, is the region most important for determining thermal rate constants, but at low energy quantum effects are expected to be significant, hence the desire for a rigorous *quantum* analogue of classical TST. Although this quest has had some useful byproducts (e.g., semiclassical versions of TST,[9] including the "instanton" approximation[4] that has seen wide use), nothing emerged that one can properly call a rigorous quantum TST. The methodologies described in the present paper are, strictly speaking, simply quantum *simulations*, yet it will be seen that in appropriate cases, e.g., simple barrier crossing dynamics, qualitative vestiges of TST reemerge and provide a very useful interpretation even in these rigorous computational approaches. In the case of more complicated dynamics, e.g., involving formation of a long-lived collision intermediate, when TST is not an appropriate dynamical approximation, these rigorous approaches of course still apply.

Section II first sketches the basic theoretical formulation, and then sections III and IV deal with the practical implementation and applications of the microcanonical and canonical versions of the theory, respectively. Section V shows how the effects of *pressure* (within the Lindemann picture) on bimolecular reactions can be included in this rigorous formulation, and section VI concludes by discussing some approximations that can be implemented within this overall formulation.

## II. Survey of Basic Formulation

**a. Classical Mechanics.** It is useful first to consider the "direct" and "correct" way of calculating a rate constant within *classical mechanics*. A rate constant is an average of the *flux* through some dividing surface that separates reactants from products. Thus the canonical rate constant is given by

$$k_{CL}(T) = Q_r(T)^{-1} (2\pi\hbar)^{-F} \int \mathrm{d}\mathbf{p}_1 \int \mathrm{d}\mathbf{q}_1\, \mathrm{e}^{-\beta H(\mathbf{p}_1,\mathbf{q}_1)}\, F(\mathbf{p}_1,\mathbf{q}_1)\, \mathrm{P}_r(\mathbf{p}_1,\mathbf{q}_1) \tag{2.1}$$

where $(\mathbf{p}_1,\mathbf{q}_1)$ denotes the initial conditions of the momenta and coordinates for classical trajectories of the molecular system (consisting of $F$ degrees of freedom, whose classical Hamilton is $H(\mathbf{p},\mathbf{q})$). $F$ is the flux factor, which is the rate that trajectories cross the dividing surface specified by the equation

$$s(\mathbf{q}) = 0 \tag{2.2}$$

For example, $s(\mathbf{q})$ is some function of the coordinates of the system that is negative, say, on the reactant side of the dividing surface and positive on the product side. ($s$ might be one of the coordinates—the "reaction coordinate"—but it is not necessary to choose the coordinates $\mathbf{q}$ in this way.) $F$ is then given by

$$F(\mathbf{p},\mathbf{q}) = \frac{\mathrm{d}}{\mathrm{d}t} h(s(\mathbf{q})) \tag{2.3a}$$

$$= \delta(s(\mathbf{q})) \frac{\partial s}{\partial \mathbf{q}} \cdot \dot{\mathbf{q}}(t) \tag{2.3b}$$

$$= \delta(s(\mathbf{q})) \frac{\partial s}{\partial \mathbf{q}} \cdot \mathbf{p}/m \tag{2.3c}$$

where $h(\zeta)$ is the Heaviside function,

$$h(\zeta) = \begin{cases} 1 & \text{if } \zeta > 0 \\ 0 & \text{if } \zeta < 0 \end{cases} \tag{2.4}$$

That is, $h(s(\mathbf{q}))$ is the "microprobability" that the coordinate $\mathbf{q}$ lies on the product side of the dividing surface, and in eq 2.3c it has been assumed for simplicity that the coordinates are cartesian so that $\dot{\mathbf{q}} = \mathbf{p}/m$ (but this can be generalized with no essential changes). The factor $\mathrm{P}_r$ in eq 2.1 contains all the dynamical information: it is, in words, equal to 1 if the trajectory with these initial conditions is on the product side of the dividing surface in the infinite future and 0 otherwise; this can be stated algebraically as

$$\mathrm{P}_r(\mathbf{p}_1,\mathbf{q}_1) = \lim_{t\to\infty} h[s(\mathbf{q}(t))] \tag{2.5}$$

where $\mathbf{q}(t) \equiv \mathbf{q}(t; \mathbf{p}_1,\mathbf{q}_1)$, or equivalently as

$$P_r = \int_0^\infty dt \frac{d}{dt} h[s(\mathbf{q}(t))] \tag{2.6a}$$

$$= \int_0^\infty dt\, \delta[s(\mathbf{q}(t))] \frac{\partial s}{\partial \mathbf{q}} \cdot \dot{\mathbf{q}}(t) \tag{2.6b}$$

$$= \int_0^\infty dt\, F(\mathbf{p}(t),\mathbf{q}(t)) \tag{2.6c}$$

Thus $P_r(\mathbf{p}_1,\mathbf{q}_1)$, the probability that the trajectory with the indicated initial conditions lies on the product side of the dividing surface as $t \rightarrow \infty$, is given by the time integral of the time-evolved flux along the trajectory. Inserting eq 2.6c into 2.1, and interchanging the order of the phase space and time integrals, gives

$$k_{CL}(T) = Q_r(T)^{-1} \int_0^\infty dt\, C_f(t) \tag{2.7a}$$

where

$$C_f(t) = (2\pi\hbar)^{-F} \int d\mathbf{p}_1 \int d\mathbf{q}_1\, e^{-\beta H(\mathbf{p}_1,\mathbf{q}_1)} F(\mathbf{p}_1,\mathbf{q}_1)\, F(\mathbf{p}(t),\mathbf{q}(t)) \tag{2.7b}$$

That is, the rate constant is the time integral of the flux−flux autocorrelation function.

Equation 2.7 is the desired "direct" and "correct" way of calculating the thermal rate constant classically. It is "correct" because it is based on the full classical dynamics (a trajectory calculation), and no approximations are entailed in going from eq 2.1 to 2.7. It is "direct" because it requires only dynamical information about whether or not the trajectory lies on the product side of the dividing surface as $t \rightarrow \infty$; it requires no information about the product state distribution, and so forth. It therefore typically requires only short time dynamics to evaluate eq 2.7, provided the dividing surface is chosen at the most useful location. (Because of Liouville's theorem, the result for $k(T)$ is independent of the location of the dividing surface, although the correlation function $C_f(t)$ is not.)

TST, as Pechukas and McLafferty[8] emphasize, is exact classically if all trajectories that start out on the dividing surface at $t = 0$ never recross it at a later time. If this is the case, then $F(\mathbf{p}(t),\mathbf{q}(t)) \equiv \delta(s(t))\dot{s}(t)$ will be identically zero for all $t > 0$ (because $s(t)$ will never be zero if the trajectory never returns to the dividing surface), so that $C_f(t) = 0$ for all $t > 0$. To see the behavior of $C_f(t)$ for $t$ very close to 0, one makes a short-time approximation for the trajectory,

$$\mathbf{q}(t) \cong \mathbf{q}_1 + \frac{\mathbf{p}_1}{m} t$$

$$\mathbf{p}(t) \cong \mathbf{p}_1$$

and if for convenience one chooses coordinates so that $s(\mathbf{q}) = q_F$ is the reaction coordinate, then it is not a lengthy calculation to show that eq 2.7b for the correlation function gives

$$C_f(t) = \frac{kT}{h} Q^\ddagger(T)\, \delta(t)/2 \tag{2.8a}$$

where $Q^\ddagger(T)$ is the partition function of the "activated complex", the molecular system minus the $F$th degree of freedom,

$$Q^\ddagger(T) = (2\pi\hbar)^{-(F-1)} \int d\mathbf{p}' \int d\mathbf{q}'\, e^{-\beta H^\ddagger(\mathbf{p}',\mathbf{q}')} \tag{2.8b}$$

where $(\mathbf{p}',\mathbf{q}') \equiv (p_k,q_k)$, $k = 1, ..., F-1$, and $H^\ddagger(\mathbf{p}',\mathbf{q}') = \mathbf{p}'^2/2m + V(\mathbf{q}',q_F = 0)$. Thus in the limit of TST-like dynamics (no recrossing trajectories) the flux correlation function falls to zero *very* quickly, and its integral (eq 2.7a) gives the conventional TST result[7] for the rate constant

$$k_{CL\ TST}(T) = \frac{kT}{h} \frac{Q^\ddagger(T)}{Q_r(T)} \tag{2.8c}$$

**b. Quantum Mechanics.** The reason it is worthwhile to describe the classical situation in as much detail as above is that the quantum treatment follows it very closely. Thus ref 6 showed that the quantum expression for the rate constant×e2 i.e., eqs 1.2 and 1.3, can be cast in a form analogous to the classical expression eq 2.1,

$$k_{QM}(T) = Q_r(T)^{-1}\, \mathrm{tr}(e^{-\beta\hat{H}} \hat{F} P_r) \tag{2.9}$$

where $\hat{H}$, $\hat{F}$, and $P_r$ are quantum operators analogous to the classical functions in eqs 2.1, with a quantum trace replacing the classical phase space average in the usual way. Analogous to eq 2.5, for example, the operator $P_r$ is the long-time limit of the time-evolved Heaviside function,

$$P_r = \lim_{t\rightarrow\infty} e^{i\hat{H}t/\hbar} \hat{h}(s) e^{-i\hat{H}t/\hbar} \tag{2.10}$$

but now the time evolution is carried out quantum mechanically in terms of the time evolution operator $\exp(-i\hat{H}t/\hbar)$ by the usual Heisenberg prescription. One can also perform the same manipulations as in eq 2.6,

$$P_r = \int_0^\infty dt \frac{d}{dt} e^{i\hat{H}t/\hbar} \hat{h}(s) e^{-i\hat{H}t/\hbar} \tag{2.10a}$$

$$= \int_0^\infty dt\, e^{i\hat{H}t/\hbar} \frac{i}{\hbar}[\hat{H},\hat{h}] e^{-i\hat{H}t/\hbar} \tag{2.10b}$$

$$= \int_0^\infty dt\, e^{i\hat{H}t/\hbar} \hat{F} e^{-i\hat{H}t/\hbar} \tag{2.10c}$$

That is, the projection operator $P_r$ is the time integral of the quantum mechanically time-evolved flux operator,

$$\hat{F} \equiv \frac{i}{\hbar}[\hat{H},\hat{h}] \tag{2.11a}$$

$$= \frac{1}{2m}\left[\delta(s(\hat{\mathbf{q}})) \frac{\partial s}{\partial \mathbf{q}} \cdot \hat{\mathbf{p}} + \hat{\mathbf{p}} \cdot \frac{\partial s}{\partial \mathbf{q}} \delta(s(\hat{\mathbf{q}}))\right] \tag{2.11b}$$

where eq 2.11b has assumed a Cartesian Hamiltonian. Inserting eq 2.10c into 2.9, and interchanging the order of the trace and the time integral, gives the same result of eq 2.7a,

$$k_{QM}(T) = Q_r(T)^{-1} \int_0^\infty dt\, C_f(t) \tag{2.12a}$$

but where here $C_f(t)$ is the quantum flux−flux autocorrelation function,[10]

$$C_f(t) = \mathrm{tr}[e^{-\beta\hat{H}} \hat{F} e^{i\hat{H}t/\hbar} \hat{F} e^{-i\hat{H}t/\hbar}] \tag{2.12b}$$

Here I make a technical/historical digression on the operator $e^{-\beta\hat{H}}\hat{F}$ appearing in eq 2.12b; the uninterested reader may skip this paragraph. Miller, Schwartz, and Tromp (MST)[10] pointed out that the rate constant given by eq 2.12a is unchanged if the Boltzmann operator is split and sandwiched about $\hat{F}$ as follows,

$$e^{-\beta\hat{H}} \hat{F} \rightarrow e^{-\lambda\hat{H}} \hat{F} e^{-(\beta-\lambda)\hat{H}} \tag{2.13}$$

for any value of $\lambda$ between 0 and $\beta$. They made the symmetrical choice $\lambda = \beta/2$ so that the Boltzmann operator could be

combined with the time evolution operators into one "complex time" evolution operator as follows,

$$C_f^{MST}(t) = \mathrm{tr}[\hat{F}e^{i\hat{H}t_c^*/\hbar}\hat{F}e^{-iHt_c/\hbar}] \quad (2.14)$$

where $t_c = t - i\hbar\beta/2$. This was particularly useful in trying to compute $C_f(t)$ by analytic continuation methods.[11] Earlier work by Yamamoto,[12] using linear response theory,[13] also expressed the rate constant in terms of a flux−flux autocorrelation function, and his correlation function corresponds to *averaging* eq 2.13 over $\lambda$ (the Kubo transform),

$$(e^{-\beta\hat{H}}\hat{F})_{Kubo} \equiv \frac{1}{\beta}\int_0^\beta d\lambda\, e^{-\lambda\hat{H}}\hat{F}e^{-(\beta-\lambda)\hat{H}} \quad (2.15a)$$

which can be shown to be[14]

$$(e^{-\beta\hat{H}}\hat{F})_{Kubo} = \frac{i}{\hbar\beta}[\hat{h}, e^{-\beta\hat{H}}] \quad (2.15b)$$

Although the rate constants given by the MST and the Yamamoto correlation functions are the same, the correlation functions are different, particularly so at short time, where Yamamoto's is singular. One can see this explicitly by carrying out the calculation analytically for the free particle case. MST show that their correlation function for this TST-like case is

$$C_f^{MST}(t) = \frac{kT}{h}\frac{(\hbar\beta/2)^2}{[t^2 + (\hbar\beta/2)^2]^{3/2}} \quad (2.16)$$

A similar calculation for Yamamoto's correlation function—that is, using eq 2.15b rather than $e^{-\beta\hat{H}/2}\hat{F}e^{-\beta\hat{H}/2}$—gives

$$C_f^{Y}(t) = \frac{kT}{h}\frac{1}{\hbar\beta}\frac{(\sqrt{t^2 + (\hbar\beta)^2} - t)^{3/2}}{\sqrt{2}t\sqrt{t^2 + (\hbar\beta)^2}} \quad (2.17)$$

Both eq 2.16 and eq 2.17 integrate to give $kT/h$, as they must, and for long time they both behave as

$$\lim_{t\to\infty} C_f(t) \sim \frac{kT}{h}\left(\frac{\hbar\beta}{2}\right)^2/t^3 \quad (2.18)$$

For short time, however, they differ:

$$\lim_{t\to 0} C_f^{MST}(t) = \frac{kT}{h}\frac{2}{\hbar\beta}\left[1 - \frac{3}{2}\left(\frac{2t}{\hbar\beta}\right)^2\right] \quad (2.19a)$$

while

$$\lim_{t\to 0} C_f^{Y}(t) = \frac{kT}{h}\frac{1}{\hbar\beta}\left(\frac{\hbar\beta}{2t}\right)^{1/2} \quad (2.19b)$$

Although the singularity at $t = 0$ in eq 2.19b is integrable, it is obviously very undesirable for numerical calculations, which must be careful to describe this important contribution to the time integral correctly.

The microcanonical rate expression, i.e., the quantum expression for the cumulative reaction probability $N(E)$, is essentially the same as eq 2.9 with the replacement of the Boltzmann operator $e^{-\beta\hat{H}}$ by the microcanonical density operator $\delta(E - \hat{H})$,

$$N(E) = 2\pi\hbar\,\mathrm{tr}[\delta(E - \hat{H})\hat{F}P_r] \quad (2.20)$$

By making use of the operator identity

$$\int_{-\infty}^{\infty} dE\, e^{-\beta E}\,\delta(E - \hat{H}) = e^{-\beta\hat{H}} \quad (2.21)$$

it is easy to see that this definition of $N(E)$, and eq 1.3b giving $k(T)$ in terms of $N(E)$, immediately recovers the quantum expression for $k(T)$ in eq 2.9.

By using eq 2.10c for the projection operator $P_r$, a very interesting expression can be obtained for $N(E)$,

$$N(E) = (2\pi\hbar)\frac{1}{2}\int_{-\infty}^{\infty} dt\,\mathrm{tr}[\delta(E - \hat{H})\hat{F}e^{i\hat{H}t/\hbar}\hat{F}e^{-i\hat{H}t/\hbar}] \quad (2.22a)$$

where the time integral has been changed from $(0,\infty)$ to $(-\infty,\infty)$ (and divided by 2) since the integrand is an even function of $t$. Since the right-most time evolution operator in eq 2.22a sits next to $\delta(E - \hat{H})$ (with a cyclic permutation of operators in the trace), one can make the replacement $e^{-i\hat{H}t/\hbar} \rightarrow e^{-iEt/\hbar}$, and then this scalar phase factor is combined with the other time evolution operator, to give

$$N(E) = (2\pi\hbar)\frac{1}{2}\int_{-\infty}^{\infty} dt\,\mathrm{tr}[\delta(E - \hat{H})\hat{F}e^{i(\hat{H}-E)t/\hbar}\hat{F}] \quad (2.22b)$$

The time integral can then be evaluated using the Fourier representation of the delta function,

$$\int_{-\infty}^{\infty} dt\, e^{i(\hat{H}-E)t/\hbar} = 2\pi\hbar\,\delta(E - \hat{H})$$

so that one obtains the following result,[10]

$$N(E) = \frac{1}{2}(2\pi\hbar)^2\,\mathrm{tr}[\delta(E - \hat{H})\hat{F}\,\delta(E - \hat{H})\,\hat{F}] \quad (2.23)$$

showing that the calculation of $N(E)$ requires only that one have a way to evaluate the microcanonical density operator.

## III. Microcanonical Case

**a. Practical Implementation.** Thirumalai et al.[15] suggested one interesting way to represent the microcanonical density operator for use in eq 2.23, namely, a Gaussian prelimit representation of the delta function,

$$\delta(E - \hat{H}) = \left(\frac{\alpha}{\pi}\right)^{1/2} e^{-\alpha(\hat{H}-E)^2} \quad (3.1)$$

for $\alpha$ sufficiently large. To evaluate the exponential operator, they used a Magnus-type expansion,

$$e^{-\alpha(\hat{H}-E)^2} = \prod_{n=1}^{N} e^{-\Delta\alpha(\hat{H}-E)^2} \quad (3.2)$$

where $\Delta\alpha = \alpha/N$, and if $\Delta\alpha$ is sufficiently small, simple approximations for each factor in eq 3.2 are possible. One may also think of eq 3.1 arising from the Fourier time integral representation of the delta function,

$$\delta(E - \hat{H}) = \frac{1}{2\pi\hbar}\int_{-\infty}^{\infty} dt\, e^{-t^2/4\alpha\hbar^2} e^{i(E-\hat{H})t/\hbar} \quad (3.3)$$

where a Gaussian convergence factor has been inserted into the integrand to damp the $t \rightarrow \pm\infty$ regions. Equation 3.3 gives eq 3.1, and it is again clear that the $\alpha \rightarrow \infty$ limit yields the formally exact delta function.

A more standard way of cutting off the time integral in the Fourier representation of the delta function is to use an exponential convergence factor: thus the integral representation

$$\delta(E-\hat{H}) = \frac{1}{2\pi\hbar}\int_{-\infty}^{\infty} dt\, e^{i(E-\hat{H})t/\hbar} \tag{3.4a}$$

$$= \frac{1}{\pi\hbar}\mathrm{Re}\int_{0}^{\infty} dt\, e^{i(E-\hat{H})t/\hbar} \tag{3.4b}$$

is modified by inserting the factor $e^{-\epsilon t/\hbar}$ into the integrand,

$$\delta(E-\hat{H}) = \frac{1}{\pi\hbar}\mathrm{Re}\int_{0}^{\infty} dt\, e^{-\epsilon t/\hbar} e^{i(E-\hat{H})t/\hbar} \tag{3.4c}$$

which damps the long-time behavior. This integral can be formally evaluated to give the standard expression

$$\delta(E-H) = -\frac{1}{\pi}\mathrm{Im}\,\hat{G}_{\epsilon}(E) \tag{3.5a}$$

where $\hat{G}_{\epsilon}(E)$ is the prelimit Green's function,

$$\hat{G}_{\epsilon}(E) = (E + i\epsilon - \hat{H})^{-1} \tag{3.5b}$$

The energy parameter $\epsilon$ is obviously required to be positive, and the limit $\epsilon \rightarrow 0$ is taken at some appropriate stage to obtain the formally exact result. Equations 3.5a and 3.5b can be combined to express $\delta(E-\hat{H})$ as

$$\delta(E-\hat{H}) = \frac{\epsilon}{\pi}[\epsilon^2 + (\hat{H}-E)^2]^{-1} \tag{3.6}$$

showing that it is a Lorentzian prelimit representation of the delta function.

A much more effective way[16] to represent the Green's function and density operator, however, is to take $\epsilon$ in eq 3.5 to be an *absorbing potential* $\epsilon(\mathbf{q})$. This idea was motivated by the negative imaginary potential that is added to the true potential energy function,

$$V(\mathbf{q}) \rightarrow V(\mathbf{q}) - i\epsilon(\mathbf{q}) \tag{3.7}$$

in time-dependent wave packet calculations[17] to prevent reflections from the edge of the grid on which the wave function is represented; the negative imaginary potential in eq 3.7 is clearly a coordinate-dependent generalization of the positive constant in eq 3.5. Allowing $\epsilon$ to be a (positive) function of coordinates, i.e., a potential energy operator, is much better than taking it to be a constant, because it can be chosen to be zero in the physically relevant region of space and only "turned on" at the edges of this region to impose the outgoing wave boundary condition. Absorbing flux in this manner, and thus not allowing it to return to the interaction region, is analogous to the practice in a classical calculation of terminating trajectories as soon as they exit the interaction region.

Figure 1 shows a sketch of the potential energy surface for the generic reaction $H + H_2 \rightarrow H_2 + H$, with the absorbing potential $\epsilon(\mathbf{q})$ indicated by dashed contours. $\epsilon(\mathbf{q})$ is zero in the transition-state region, where the reaction dynamics (i.e., tunneling, recrossing dynamics) takes place, and is turned on outside this region. In practice one chooses the interaction region (the area between the absorbing potentials) to be as small as possible, so that as small a basis set as possible can be used to represent the operators and evaluate the trace. Choosing it too small, though, will cause the absorbing potentials to interfere with reaction dynamics one is attempting to describe.

With the microcanonical density operator given by eq 3.5 (with an appropriate choice for $\epsilon$), straightforward algebraic manipulations (also using eq 2.11a) lead to the following even simpler form for the cumulative reaction probability,[16b]

$$N(E) = 4\,\mathrm{tr}[\hat{G}^{+}(E)^{*}\hat{\epsilon}_{p}\hat{G}^{+}(E)\hat{\epsilon}_{r}] \tag{3.8a}$$

where $\epsilon_r$ ($\epsilon_p$) is the part of the adsorbing potential in the reactant (product) valley, and $\epsilon \equiv \epsilon_r + \epsilon_p$. This expression may be evaluated in any convenient basis set that spans the interaction region and also extends some ways into the absorbing region. The explicit matrix expression is then

$$N(E) = 4\,\mathrm{tr}[(E + i\epsilon - \mathbf{H})^{-1}\epsilon_{p}(E - i\epsilon - \mathbf{H})^{-1}\epsilon_{r}] \tag{3.8b}$$

with

$$\epsilon = \epsilon_r + \epsilon_p \tag{3.8c}$$

It is interesting to note that in eq 3.8 all reference to a specific dividing surface has vanished; it is implicit that a dividing surface lies somewhere between the reactant and product absorbing potentials (cf. Figure 1), but there is no dependence on its specific choice. This is just as it should be, for as noted above these formally exact rate expressions are invariant to the choice of the dividing surface.

In recent calculations it has furthermore been shown[18] that an extremely efficient way to evaluate the trace in eq 3.8 is to symmetrize the matrix inside the trace operation as follows,

$$N(E) = \mathrm{tr}[\hat{P}(E)] \tag{3.9a}$$

where

$$\hat{P}(E) \equiv 4\hat{\epsilon}_{r}^{1/2}\hat{G}(E)^{*}\hat{\epsilon}_{p}\hat{G}(E)\hat{\epsilon}_{r}^{1/2} \tag{3.9b}$$

$\hat{P}(E)$ is seen to be a Hermitian operator (or matrix), so that its eigenvalues $\{p_k(E)\}$ are all real, and from eq 3.9a the CRP is their sum,

$$N(E) = \sum_{k} p_k(E) \tag{3.10}$$

It is also easy to see that $\hat{P}(E)$ is a positive operator, so that its eigenvalues are all positive. It is not as obvious—but can be readily shown[16]—that $\hat{P}(E)$ is also bounded by their identity operator

$$\hat{P}(E) \leq 1 \tag{3.11a}$$

from which it follows that

$$0 \leq p_k(E) \leq 1 \tag{3.11b}$$

The eigenvalues $\{p_k\}$ can thus be thought of as *probabilities*, and then eq 3.10—which gives the *exact* $N(E)$ as the sum of these "eigen reaction probabilities"—bears an interesting resemblance to the simple transition-state approximation in which $N(E)$ is given as a sum of one-dimensional tunneling (or transmission) probabilities over all states of the activated complex.

The pragmatic reason for focusing on the *reaction probability operator/matrix* $\hat{P}(E)$ defined by eq 3.9 is that it is of *low rank*; that is, the number of its eigenvalues $\{p_k(E)\}$ that are significantly different from zero is very small (compared to the dimension of its matrix representation); the number of its nonzero eigenvalues is approximately the number of states of the activated complex of TST that are energetically accessible at total energy $E$. This means that a Lanczos iteration procedure applied to $\hat{P}(E)$ is extremely efficient for determining its nonzero eigenvalues, the number of such iterations being essentially the number of nonzero eigenvalues, and this in turn minimizes the

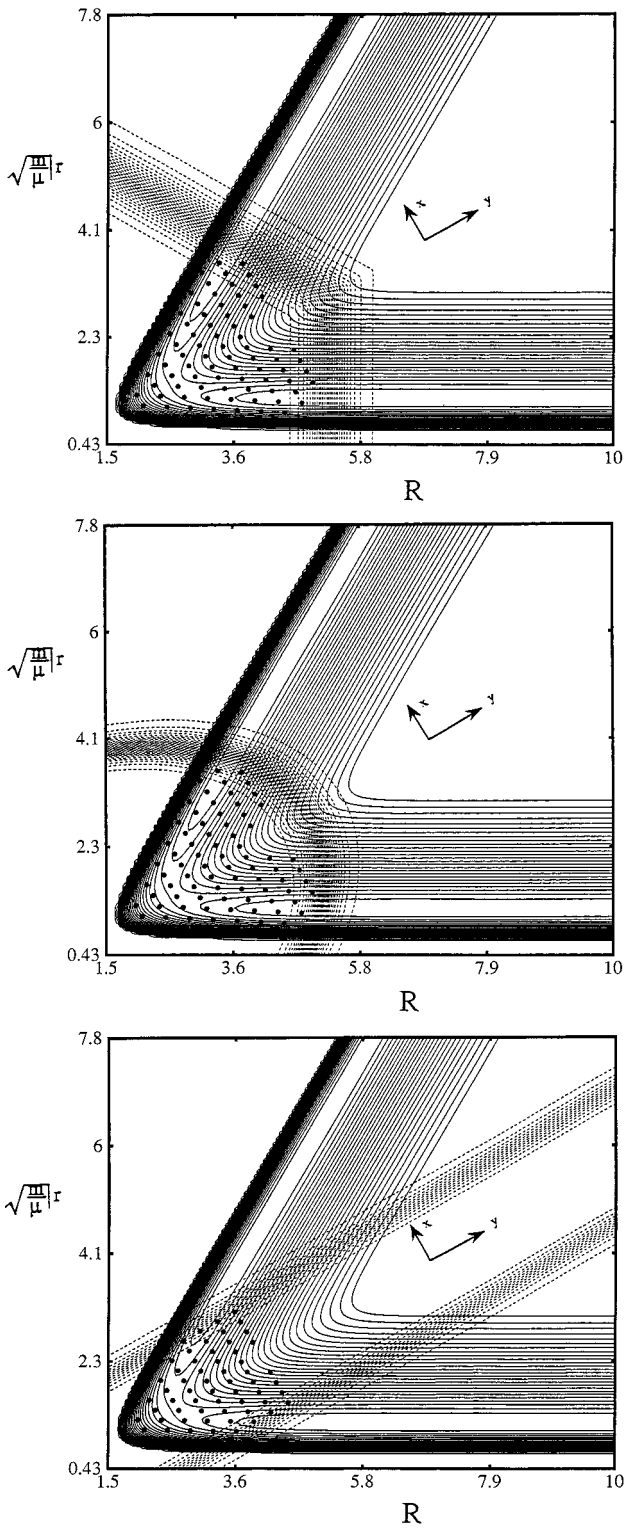


**Figure 1.** Contour diagram of the potential energy surface for the collinear $H + H_2 \rightarrow H_2 + H$ reaction. The dashed lines are contours of the absorbing potential $\epsilon(\mathbf{q})$ (which is zero in the interaction region) for three different choices of it; they all work essentially equally well. The points are the coordinate grid for the discrete variation representation of the Hamiltonian and other operators.

overall number of operations of the Greens function that are required. (Another, very tantalizing, way to find the eigen reaction probabilities is to determine the eigenvalues of the matrix $\hat{P}(E)^{-1} \equiv {}^1/_4\hat{\epsilon}_r^{-1/2}(E + i\hat{\epsilon} - \hat{H})\hat{\epsilon}_p^{-1}(E - i\hat{\epsilon} - \hat{H})\hat{\epsilon}_r^{-1/2}$, which are clearly the values $\{1/p_k\}$. The operator $\hat{P}(E)^{-1}$ requires *no* Green's function operators, but there are numerical

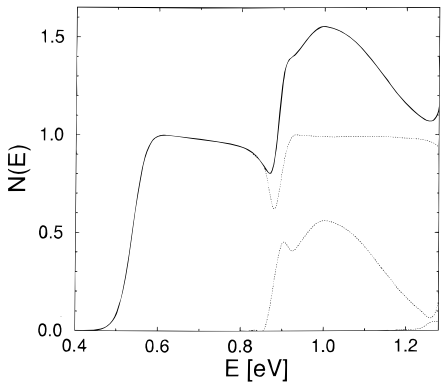


**Figure 2.** The cumulative reaction probability $N(E)$ (solid line) and the individual eigenvalues of $\hat{P}$ (dotted lines) as a function of energy (in electronvolts) for the collinear $H + H_2$ reaction.

difficulties due to the reciprocals of the absorbing potentials that occur in it. This approach does work,[18,19] however, and bears further consideration because so little effort is required to construct the matrix $\hat{P}^{-1}$.)

Equations 3.8−3.10 thus provide a practical scheme for determining the rate constant for a chemical reaction "*directly*" and "*correctly*". This is not a transition-state "theory" since calculation of the Green's function, the matrix inverse of $(E + i\epsilon - \mathbf{H})$, is equivalent to solving the Schrödinger equation; that is, it generates the complete quantum dynamics. Since this is required only in the transition-state region (between the reactant and product absorbing strips), one may think of this quantum mechanical calculation as the analogue of a classical trajectory calculation which begins trajectories on a dividing surface in the transition-state region and follows them for a short time to see which ones are reactive.

Finally, it should be noted that Zhang and Light[20] and Manthe[21] have recently described alternate ways of evaluating eq 2.23 that are based on Fourier transforming a time-dependent solution of the Schrödinger equation. This is an attractive approach because it has the capability of determining $N(E)$ for many different values of $E$ within one overall calculation.

**b. Applications.** In recent applications[16−18] it has proved useful to employ a set of *grid points* in coordinate space as the basis set in which to evaluate eq 3.8b or eqs 3.9 and 3.10. These grid, or discrete variable, methods[22−24] are proving quite useful for a variety of molecular quantum mechanical calculations. The primary advantages of such approaches are that (1) no integrals are required in order to construct the Hamiltonian matrix (e.g., the potential energy matrix is diagonal, the diagonal values being the values of the potential energy function at the grid points), and (2) the Hamiltonian matrix is extremely sparse (so that large systems of linear equations can be solved efficiently).

Figure 1 shows the set of grid points and several possible choices for the absorbing potentials which yield accurate results[16] for the standard test problem, the collinear $H + H_2 \rightarrow H_2 + H$ reaction. The important feature to see here is how close the absorbing potentials can be brought in and how localized the grid can be taken about the transition-state region. This is the region in which it is necessary to determine the quantum dynamics in order to obtain the correct result for $N(E)$ (and thus $k(T)$). No information about reactant and product quantum states is involved in the calculation.

Figure 2 shows the eigen reaction probabilities $\{p_k(E)\}$ obtained[16a] for the collinear $H + H_2 \rightarrow H_2 + H$ reaction and their sum, $N(E)$. In this case about ∼100−200 grid points are needed to span the interaction region, and this is therefore the dimension of all the matrices of $\hat{H}$, $\hat{G}(E)$, $\hat{P}(E)$, and so forth, in

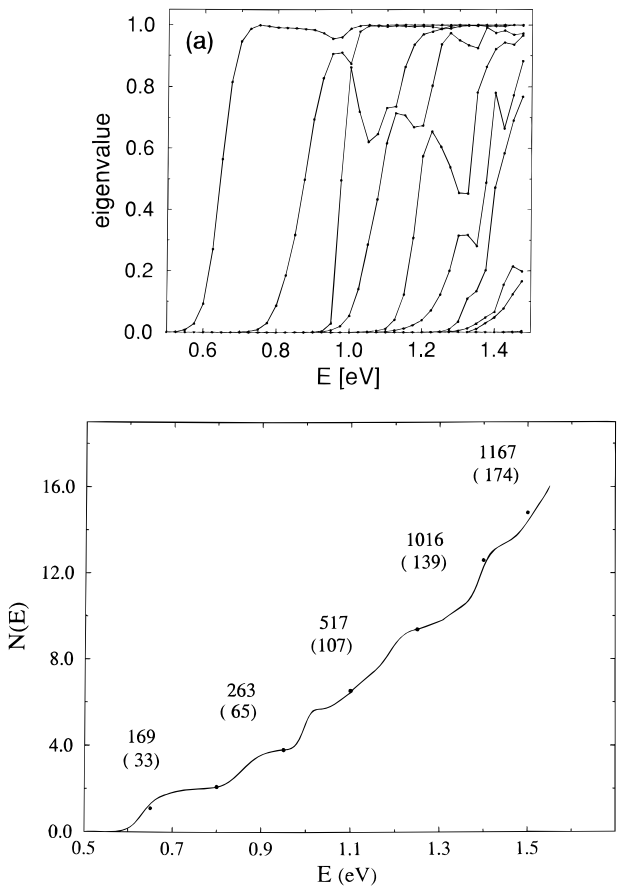


**Figure 3.** (a) Eigen reaction probabilities $\{p_k(E)\}$ for the three-dimensional H + $H_2$ reaction (for $J = 0$), as a function of total energy. (b) The cumulative reaction probability $N(E) = \sum_k p_k(E)$.

the grid or discrete variable representation. As seen in Figure 2, though, the number of nonzero eigen reaction probabilities—i.e., the rank of $\hat{P}(E)$ and the number of Lanczos iterations required to obtain these eigenvalues—is very small ($\leq 3$) over this entire region, and this is what makes the procedure described above so efficient.

One can qualitatively identify the individual eigen reaction probabilities in Figure 2 with the various states of the activated complex of transition-state theory. In TST each $p_k(E)$ would rise from 0 to 1 at the energy of the corresponding state of the activated complex (and stay at 1 for all higher energies); the deviations from this behavior seen in Figure 2 are due to TST-violating dynamics, i.e., recrossing trajectories in a classical picture, and the result of a short-lived collision complex that causes resonances in a quantum description. $N(E)$ would be a monotonically increasing function of $E$ if there were no recrossing flux through the interaction region, and Figure 2 shows strong deviations from this behavior.

Figure 3a,b shows the corresponding eigen reaction probabilities and CRP for the three-dimensional version[16b] of the H + $H_2$ reaction (for total angular momentum $J = 0$). Even though collision complexes are also formed in the three-dimensional version of this reaction, $N(E)$ appears in Figure 3b to be monotonically increasing with energy in TST-like fashion; thus monotonicity of $N(E)$ does not guarantee that the underlying dynamics is TST-like. One also sees in Figure 3b a remnant of the staircase structure[25] in $N(E)$ that results from quantization of the states of the activated complex in TST; this survives because the eigen reaction probabilities, at least at low energies, are not overlapping; that is, $p_1(E)$ rises approximately from 0 to 1 before $p_2(E)$ begins to turn on, and so forth.

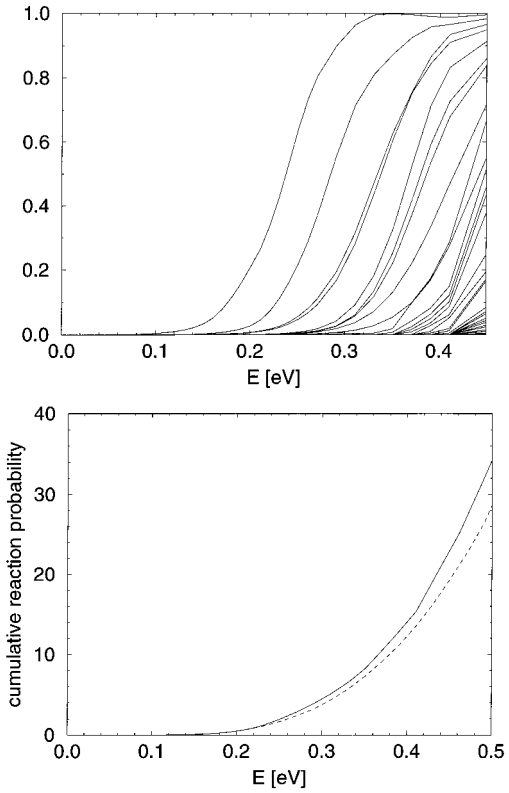


**Figure 4.** (a) Eigen reaction probabilities $\{p_k(E)\}$ for the three-dimensional $H_2$ + OH → $H_2O$ + H reaction (for $J = 0$), as a function of energy. (b) The cumulative reaction probability $N(E) = \sum_k p_k(E)$ for this reaction.

Figure 4a,b shows the eigen reaction probabilities and CRP for the first full dimensional calculation[26] of the reaction dynamics of any four-atom reaction, namely,

$$H_2 + OH \rightarrow H + H_2O \tag{3.12}$$

(There have subsequently been state-to-state reactive scattering calculations[27,28] for this reaction for some initial states, though not a complete set of them that would be required to obtain the CRP from eq 1.2.) The dynamics here is quite TST-like, as seen from the eigen reaction probabilities in Figure 4a. Here, moreover, one sees that the staircase structure in $N(E)$ has disappeared in Figure 4b. This is readily understood from Figure 4a, because the higher density of states in this six degrees of freedom system causes the eigen reaction probabilities to overlap; that is, $p_1(E)$ has not fully turned on before $p_2(E)$ begins to turn on, and so forth. The net result is that $N(E)$ has a very smooth "classical" TST look to it, although all of the tunneling corrections, corner-cutting dynamics, and so on, are being described exactly correctly.

The above examples all pertain to bimolecular reactions. A unimolecular reaction of considerable interest is the isomerization of ketene studied by Lovejoy and Moore,[29]

$$H_2C'{=}C{=}O \leftrightarrow O{=}C'{=}CH_2 \tag{3.13}$$

where C and C′ are $^{12}C$ and $^{13}C$, respectively. Figure 5a shows a schematic of the potential energy surface for the reaction, indicating that the intermediate oxirene,

is a local minimum on the PES. By very clever experimental techniques Lovejoy and Moore were able to determine the microcanonical rate $k(E)$ for reaction 3.13 with very high energy resolution and, quite remarkably, observed structure that they interpreted as resonance tunneling via the intermediate metastable states of oxirene. Calculations of $k(E)$ for this isomerization were thus undertaken[30] to lend support (or not) to this interpretation of the observed structure. Absorbing potentials (indicated by the dotted lines in Figure 5a) were located just outside the transition-state regions connecting oxirene to the two deep ketene potential minima. The isomerization dynamics deals with flux from one absorbing region to the other and thus avoids having to describe the highly excited vibrational motion in the ketene wells themselves; this is somewhat analogous to the procedure in a classical simulation of terminating the trajectories once they are past the transition region.

Even with this limited treatment of the dynamics, however, it is not possible to carry out the calculation in its full dimensionality of $F = 3N - 6 = 9$ degrees of freedom (with total angular momentum $J = 0$). We thus carried out a CRP calculation including $f$ degrees of freedom, yielding $N_f(E)$, and then folded in the other uncoupled degrees of freedom by microcanonical convolution,

$$N(E) = \sum_{\mathbf{n}=0}^{\infty} N_f(E - \epsilon_{\mathbf{n}}^{F-f}) \tag{3.15a}$$

where $\{\epsilon_{\mathbf{n}}^{F-f}\}$ are the energy levels—approximated as harmonic oscillators—for the $F - f$ uncoupled degrees of freedom; that is, $\mathbf{n} = n_{f+1}, ..., n_F$, and

$$\epsilon_{\mathbf{n}}^{F-f} = \sum_{j=f+1}^{F} \hbar\omega_j\left(n_j + \frac{1}{2}\right) \tag{3.15b}$$

This is the idea of "reduced dimensionality" approximations[31] and for $f = 1$ is the standard expression for one-dimensional tunneling corrections to microcanonical transition-state theory.[8]

Figure 5b shows results[30] obtained for $k(E)$ via the methods described above, compared to the experimental results[29] (dotted line). There is no pretense of being able to match up individual structures between the two—the potential energy surface is much too uncertain for this—but one does see that the structure obtained in the theoretical calculations is quite comparable to that seen experimentally, lending strong support to Lovejoy and Moore's interpretation.

Finally, it should be noted that the methodology described in section IIIa for calculating the cumulative reaction probability can be used for other physical processes than chemical reactions. For the transmission of electrons through a complex medium, for example, $N(E)$ is proportional to the transmitted current (here eq 1.2, with $J \equiv 0$ and multiplied by some physical constants, is known as the Landauer formula[32]), and Nitzan et al.[33] have recently using eqs 3.8, and so on, to compute the electron tunneling current through ordered molecular layers. Similarly, Peskin, Moiseyev, et al.[34] have used this approach to calculate the transmission properties of light in optical fibers which have arbitrary (and strong) variation in their index of refraction distribution.

## IV. Canonical Case

If one has determined $N(E)$ over a sufficiently wide range of energy, then the thermal (or canonical) rate constant $k(T)$ is readily obtainable over some range of temperatures $T$ via eq

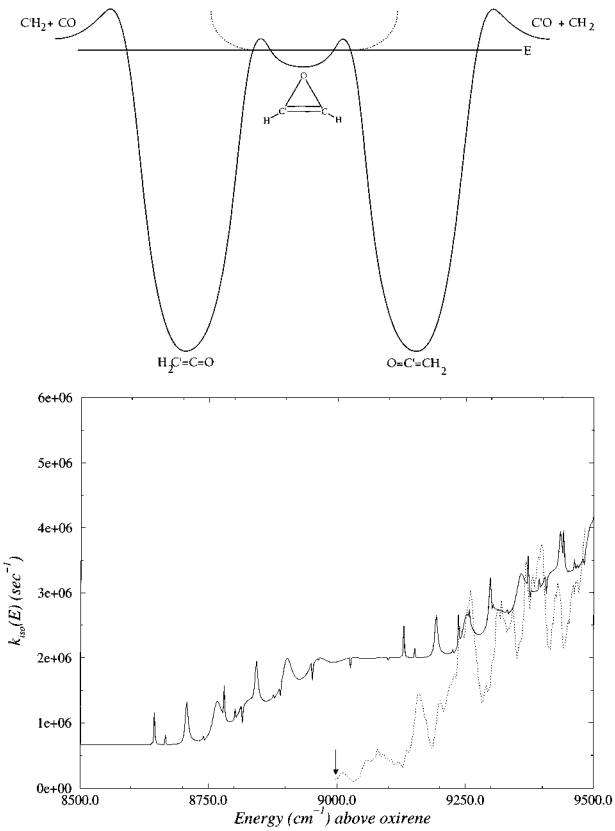


**Figure 5.** (a) Sketch of the potential energy surface for ketene isomerization, indicating the oxirene intermediate. The dotted lines indicate the location of the absorbing potential for the calculation of the isomerization rate. (b) Isomerization rate is a function of energy. The dotted line is the experimental result of ref 29 (which cuts off at the indicated energy for experimental reasons), and the solid line is the reduced dimensional calculation, eq 3.15, using three active degrees of freedom.

1.3b. This may often be the preferred way to proceed, and it is indeed true that $N(E)$ has more dynamical information in it than $k(T)$, and this can be useful for physical interpretations. However, if one is interested in obtaining $k(T)$ for one (or a few) values of $T$, then it is clearly desirable to be able to compute $k(T)$ directly for this value of $T$. The methodology for doing this is based on the expression for $k(T)$ in terms of the flux correlation function, eq 2.12.

**a. Practical Implementation.** The particular form of the flux correlation function we currently find most useful is[35]

$$C_f(t) = \mathrm{tr}[\hat{F}(\beta)e^{i\hat{H}t/\hbar}\hat{F}e^{-i\hat{H}t/\hbar}] \tag{4.1a}$$

where $\hat{F}(\beta)$ is the "Boltzmannized" flux operator,

$$\hat{F}(\beta) \equiv e^{-\beta\hat{H}/2}\hat{F}e^{-\beta\hat{H}/2} \tag{4.1b}$$

The key to efficient evaluation of the above trace is identifying some operator of low rank to exploit in a manner analogous to what was done for the microcanonical case in eqs 3.9−3.11. Here that operator is $\hat{F}(\beta)$, the rank (i.e., number of nonzero eigenvalues) of which is effectively twice the number of states of the activated complex that are thermally accessible at temperature $T$. A Lanczos iteration procedure is thus very efficient for determining these eigenvalues $\{f_n\}$ and eigenvectors $\{|v_n\rangle\}$ of $\hat{F}(\beta)$. The trace in eq 4.1a is then carried out in this representation, giving the following result for the flux correlation function,[35]

$$C_f(t) = \sum_n f_n \langle v_n(t)|\hat{F}|v_n(t)\rangle \tag{4.2a}$$

where $\{|v_n(t)\rangle\}$ are the time-evolved eigenvectors,

$$|v_n(t)\rangle \equiv e^{-i\hat{H}t/\hbar}|v_n\rangle \tag{4.2b}$$

Our group has used the split-operator algorithm to generate the time evolution in eq 4.2b (and also the action of the Boltzmann operator $e^{-\beta\hat{H}/2}$ in the Lanczos iteration of $\hat{F}(\beta)$), but other methods of "wave packet propagation" could also be used.

At this point it should be noted that the above approach has some features in common with important contributions that Light et al.[36] and Manthe et al.[37] have independently made to the efficient calculation of $k(T)$. Also related to these is earlier work by Metiu et al.[38] on calculating flux correlation functions where the properties of the Boltzmannized flux operator were exploited. The primary feature of the present methodology is that it minimizes the number of actions of the time evolution operator that are required. Note also the "conservation of effort" of this canonical version of the methodology compared to the microcanonical version described in section IIIa: to evaluate $C_f(t)$ via eq 4.2 requires the action of the time evolution operator exp(-i$\hat{H}t/\hbar$) on all eigenvectors $|v_n\rangle$ with nonzero eigenvalues $f_n$, and this is about twice the number of states of the activated complex that are thermally accessible at temperature $T$. The microcanonical calculation of $N(E)$ via eqs 3.9−3.11 requires two actions of the Green's function $\hat{G}(E) \equiv (E + i\hat{\epsilon} - \hat{H})^{-1}$ for each Lanczos iteration of operator $\hat{P}(E)$ and the number of state of the activated complex that are *energetically* accessible at energy $E$. The canonical and microcanonical versions of the methodology thus require comparable numbers of action of the time evolution operator and Green's function, respectively, which are essentially the same degree of effort since they are related as follows,

$$\hat{G}(E) = (i\hbar)^{-1}\int_0^\infty dt\, e^{i(E+i\hat{\epsilon}-\hat{H})t/\hbar} \tag{4.3}$$

**b. Applications.** Figure 6 shows the flux correlation function for the reaction[39]

$$Cl + H_2 \rightarrow HCl + H \tag{4.4}$$

for $J = 0$ total angular momentum for $T = 300$ °K and $T = 1500$ °K. The dynamics here is basically simple TST-like barrier crossing dynamics, so the correlation function looks qualitatively similar to the free-particle result, eq 2.16; for example, it falls effectively to zero by $t \cong \hbar\beta$, which is 27 f for $T = 300$ °K. At the higher temperature one does see the onset of some non-TST dynamics, i.e., recrossing flux that is typical at higher energies where some trajectories (in classical language) have so much energy that they rebound back across the dividing surface.

Figure 7 shows the results of a similar calculation (also for $J = 0$) for the reaction[35]

$$O + HCl \rightarrow OH + Cl \tag{4.5}$$

and here though the reaction dynamics is also "direct"—i.e., the correlation function falls to ~0 in a time of ~$\hbar\beta$—there is recrossing behavior in $C_f(t)$ due to the heavy + light-heavy nature of the kinematics in this reaction that is well-known to cause recrossing of the transition-state dividing surface.

**c. Treatment of $J > 0$.** The applications discussed above (including the microcanonical examples in section IIIb) have all been for zero total angular momentum ($J = 0$), which is the simplest case since there are only $3N-6$ coupled internal degrees of freedom ($N$ = number of atoms of the complete molecular system). The $J > 0$ calculation[39] is more difficult because there is an additional coupled degree of freedom, the component of total angular momentum along a body-fixed axis, and the number of states associated with this degree of freedom (the K- or Ω-states) grows with $J$ as $(2J + 1)$. Furthermore, one must carry out the calculation for many values of $J$; that is, the cumulative reaction probability and thermal rate constant are given by

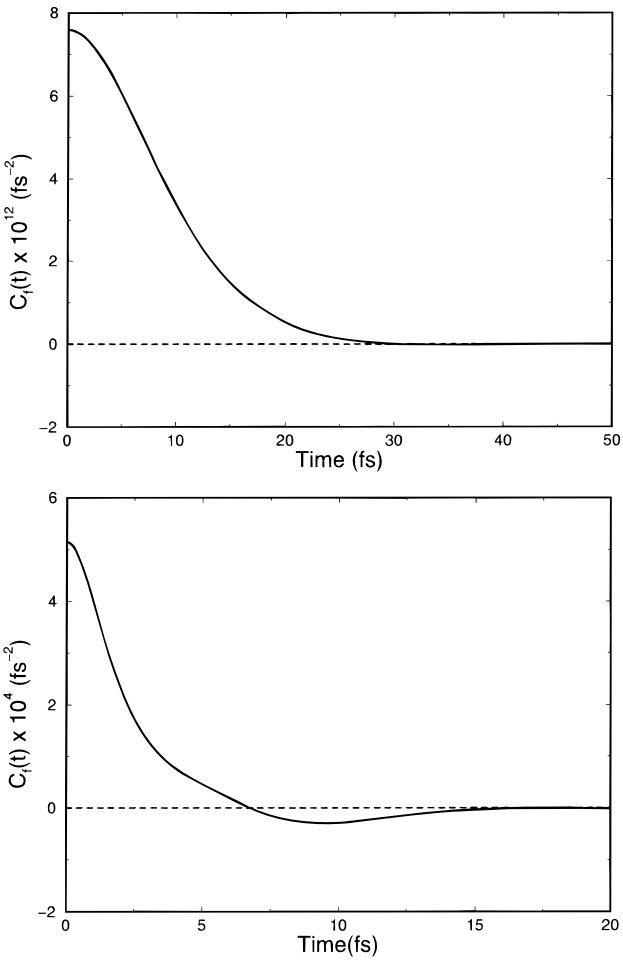


**Figure 6.** Flux−flux autocorrelation function for the Cl + $H_2$ → HCl + H reaction (in 3D, $J = 0$) for (a) $T = 300$ °K and (b) $T = 1500$ °K.

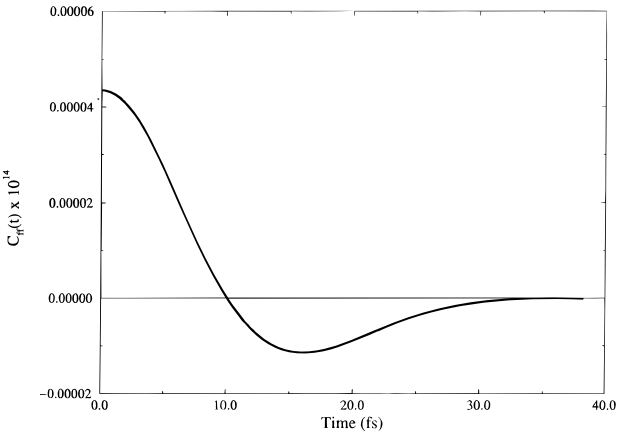


**Figure 7.** Flux−flux autocorrelation function for the O + HCl → OH + Cl reaction, for $T = 300$ °K.

$$N(E) = \sum_{J=0} (2J+1) N_J(E) \tag{4.5a}$$

$$k(T) = \sum_{J=0} (2J+1) k_J(T) \tag{4.5b}$$

where the calculation of $N_J(E)$ and $k_J(T)$ is a separate calculation of the type described above for each $J$. (The $2J + 1$ factor in eq 4.5 is from the sum over $M_J$, the projection quantum number of total angular momentum onto a space-fixed axis, on which the dynamics in field-free space does not depend.)

In reality the situation is not quite so bleak as suggested above. First, though the body-fixed projection quantum number $K$ ranges from $-J$ to $+J$, typically only small values of $K$ contribute significantly to the rate constant, e.g., $-K_{max} < K < K_{max}$, even for large $J$, so that in practice the size of the basis set does not continue to grow as $J$ increases. (This is particularly true if the body-fixed quantization axis is chosen so that the moment of inertia about it is as *small* as possible.) Second, the dependence of $k_J(T)$ (and analogously $N_J(E)$) on $J$ is often very simple and smooth—within the "$J$-shifting approximation (vide infra), for example, $\ln k_J(T)$ is a linear function of $J(J + 1)$—so that separate calculations for widely spaced values of $J$ can be carried out and then used to interpolate in order to carry out the sum in eq 4.5.

Finally, there are simple approximations for $J > 0$ that appear often to be quite accurate. One of the most promising of these a helicity-conserving approximation (HCA) based on the instantaneous principle axes (PA) of the molecular system. (McCurdy and Miller[40] suggested this in an obscure publication, and Qi and Bowman[41] later came upon it independently—terming it the "adiabatic rotation" approximation—and have demonstrated its usefulness and reliability in several different applications.) Here the $J > 0$ Hamiltonian is that for $J = 0$ with the addition of a generalized centrifugal potential,

$$\hat{H}_J = \hat{H}_{J=0} + E_{rot}^{JK}(\mathbf{q}) \tag{4.6a}$$

where $E_{rot}^{JK}$ is the energy of a rigid molecule (whose geometry is determined by the $3N-6$ internal coordinates $\mathbf{q}$) within the usual symmetric top approximation,

$$E_{rot}^{JK}(\mathbf{q}) = \frac{1}{2}[A(\mathbf{q}) + B(\mathbf{q})][J(J+1) - K^2] + C(\mathbf{q})K^2 \tag{4.6b}$$

$A$, $B$, and $C$ being the three rotation constants (e.g., $A = \hbar^2/2I_A$) related to the three instantaneous principle moments of inertia of the complete molecular system. A calculation is thus carried out for each $J$ and $K$ (which is also a conserved quantum number within the HCA), a calculation equivalent in difficulty to a $J = 0$ calculation, and then

$$k_J(T) = \sum_K k_{JK}(T) \tag{4.6c}$$

and similarly for the microcanonical use. Again, typically only small values of $K$ are required, $|K| \le K_{max}$, and it is clear that $k_{JK}(T)$ depends only on $|K|$.

The simplest approximation, the "$J$-shifting" approximation,[31] corresponds to assuming that the rotation "constants" in eq 4.6b are actually constant, evaluated at some reference geometry; that is,

$$A(\mathbf{q}) \rightarrow A(\mathbf{q}^\ddagger) \equiv A^\ddagger$$

and so forth. The rotational energy is then simply a constant term in the Hamiltonian (this is an example of the "reduced dimensionality" approximation in eq 3.15 above), and for the canonical case, for example, one has

$$k(T) = k_{J=0}(T) Q_{rot}^\ddagger(T) \tag{4.7a}$$

where $Q_{rot}^\ddagger$ is the rotational partition function for a rigid molecule with the reference geometry

$$Q_{rot}^\ddagger(T) = \sum_{J,K} \exp\left\{-\beta\left[\frac{1}{2}(A^\ddagger + B^\ddagger)(J(J+1) - K^2) + C^\ddagger K^2\right]\right\} \tag{4.7b}$$

If the reference geometry is linear, then $C^\ddagger = \infty$ and eq 4.7b thus includes only $K = 0$; this is the *extreme* case where only small values of $|K|$ contribute. The $J$-shifting approximation, therefore, requires only a $J = 0$ calculation, an enormous simplification.

Figure 8a shows accurate calculations[39] of $k_J(T)$ for a range of $J$ values for the $Cl + H_2$ reaction discussed above, showing that once $J$ is larger than 3 or so, the dependence on $J$ is very simple, of the form expected from the simple $J$-shifting approximation (since $C^\ddagger = 0$ here). Figure 8b shows an Arrhenius plot of the full rate constant $k(T)$, compared to the

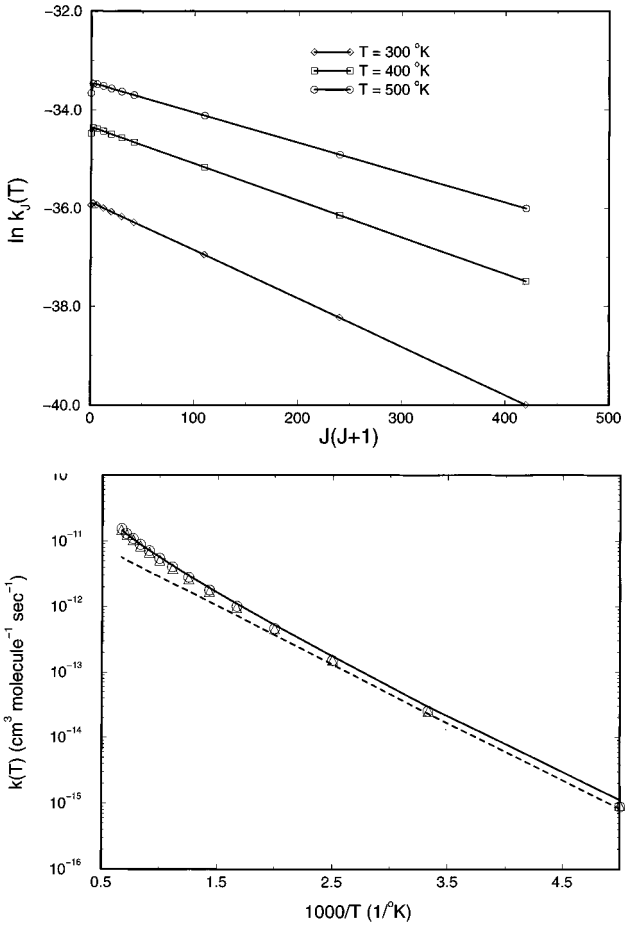


**Figure 8.** (a) $J$-dependence of $k_J(T)$ for the $Cl + H_2 \rightarrow HCl + H$ reaction, for several temperatures. (b) Arrhenius plot of the full rate constant (summed over $J$, i.e., eq 4.5b): the solid line is the exact result (i.e., with no approximation to the rotational motion), the triangles are the result of the principle axis helicity conserving approximation (which includes centrifugal distortion but not Coriolis coupling), and the dashed line is the result of the $J$-shifting approximation (i.e., an uncoupled rigid rotor approximation).

result of the simple *J*-shifting approximation and also to the HCA. The former is too small, presumably because only $K = 0$ is included,[42] and it becomes progressively worse for higher temperature, being a factor of ~2.6 too small at $T = 1500$ K; at 300 K it is ~30% too small. The HCA, however, is seen to be quite satisfactory for the entire temperature range; this is quite an encouraging state of affairs, because as discussed above, the HCA requires calculations for only a relatively small number of (*J*, *K*) values, each of which is essentially the effort of the $J = 0$ calculation.

## V. Effects of Pressure

For many chemical applications, e.g., chemical reactions in realistic combustion environments, the gas pressures are sufficiently high that bimolecular rate constants—and almost always unimolecular rate constants—are pressure-dependent. In the Lindemann description of recombination reactions (and their inverse, unimolecular dissociation), for example,

$$\mathrm{A + B} \leftrightarrow \mathrm{AB^*} \tag{5.1a}$$

$$\mathrm{AB^* + M} \rightarrow \mathrm{AB} \tag{5.1b}$$

the pressure of the "bath" gas molecules M plays a central role: the standard textbook expression[43] for the rate of the reaction A + B → AB via the mechanism of eq 5.1 is

$$k(T,\omega) = Q_\mathrm{r}(T)^{-1}\sum_l \mathrm{e}^{-\beta E_l} k_l \omega/(k_l + \omega) \tag{5.2}$$

where $\{E_l\}$ and $\{k_l\}$ are the energies and unimolecular decay rates of metastable states of the AB* complex, $\omega \equiv [\mathrm{M}]k_\mathrm{deact}$ is the frequency of "strong" (deactivating) collisions that stabilize the complex (i.e., $k_\mathrm{deact}$ is the bimolecular rate constant for the second step of the mechanism, eq 5.1b, and $\omega$ is thus proportional to the pressure of the bath gas), and $Q_\mathrm{r}(T)$ is the reactant partition function per unit volume.

Recently, however, it has been shown[44] how the flux correlation functions discussed above in sections II and IV can be used to combine a completely rigorous quantum treatment of the first step of the Lindemann reactant of eq 5.1a, i.e., the A + B collision dynamics, with the strong collision model for the deactivation step of eq 5.1b. (It is also possible to go beyond the strong collision approximation,[45] but this is considerably more complicated.) The derivation proceeds very much along the lines of that sketched in section IIa: referring to Figure 9a, which indicates a dividing surface which defines the "complex" AB* (inside of which a strong collision leads to recombination), the rate constant for recombination is given by

$$k(T,\omega) = Q_\mathrm{r}(T)^{-1}\int_0^\infty \mathrm{d}t\, C_\mathrm{f}(t)\, \mathrm{e}^{-\omega t} \tag{5.3}$$

where $C_\mathrm{f}(t)$ is the flux−flux autocorrelation function with respect to this dividing surface. Not only is eq 5.3 more accurate then eq 5.2 but it is less ambiguous. One does not have to extract individual resonance energies and widths (i.e., decay rates) from the A + B scattering matrix and decide what is a resonance and what is not; eq 5.3 includes the contribution to recombination from direct (i.e., nonresonant) A + B scattering as well as the (usually more important) contribution from complex formation (i.e., scattering resonances). Equation 5.3 also has a clean separation between the two steps of the Lindemann mechanism: the flux correlation function $C_\mathrm{f}(t)$ is a property only of the A + B scattering dynamics, eq 5.1a, while the factor $\mathrm{e}^{-\omega t}$ deals with the collisional relaxation, eq 5.1b; $\mathrm{e}^{-\omega t}$ is the probability of *not* experiencing a strong collision between time 0 and *t*.

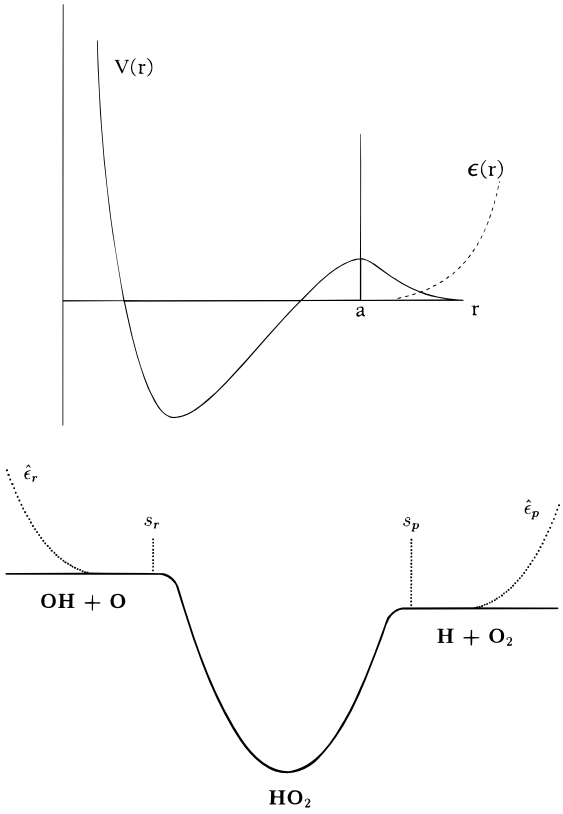


**Figure 9.** (a) Sketch of a potential energy surface for the A + B system in eq 5.1. $r = a$ is the "dividing surface" for defining the flux, and $\epsilon(r)$ is the absorbing potential used for carrying out the quantum calculation. (b) Sketch of the potential surface for the OH + O → H + $O_2$, $HO_2$ reaction and recombination. $s = s_\mathrm{r}$ and $s = s_\mathrm{p}$ indicate the two dividing surfaces, and $\epsilon_\mathrm{r}$ and $\epsilon_\mathrm{p}$ the parts of the absorbing potential in the reactant and product regions.

Qi and Bowman[46] carried out the first calculation using this theory, for the H + CO → HCO recombination, and Mandelshtam et al.[47] carried out similar calculations (though with the time-independent version of the theory) for H + $O_2$ → $HO_2$ at energies below the threshold for the O + OH channel.

More recently Germann and Miller[48] have shown how the above theoretical description of pressure effects can be generalized to include the effect of pressure on bimolecular *reactive* processes, as well as recombination, with application to

$$\mathrm{O + OH + M} \rightarrow \mathrm{HO_2 + M} \tag{5.4a}$$

$$\rightarrow \mathrm{H + O_2 + M} \tag{5.4b}$$

Again, the derivation of the rate expressions follows the same analysis as in section IIa. Referring to Figure 9b, the recombination and reaction rates are given, respectiely, by

$$k_\mathrm{recomb}(T,\omega) = Q_\mathrm{r}(T)^{-1}\int_0^\infty \mathrm{d}t\, \mathrm{e}^{-\omega t}[C_\mathrm{rr}(t) - C_\mathrm{rp}(t)] \tag{5.5a}$$

$$k_{\mathrm{p}\leftarrow\mathrm{r}}(T,\omega) = Q_\mathrm{r}(T)^{-1}\int_0^\infty \mathrm{d}t\, \mathrm{e}^{-\omega t} C_\mathrm{rp}(t) \tag{5.5b}$$

where the two flux correlation functions are

$$C_\mathrm{rr}(t) = \mathrm{tr}[\hat{F}_\mathrm{r}(\beta)\mathrm{e}^{\mathrm{i}\hat{H}t/\hbar}\hat{F}_\mathrm{r}\mathrm{e}^{-\mathrm{i}\hat{H}t/\hbar}] \tag{5.6a}$$

$$C_\mathrm{rp}(t) = \mathrm{tr}[\hat{F}_\mathrm{r}(\beta)\mathrm{e}^{\mathrm{i}\hat{H}t/\hbar}\hat{F}_\mathrm{p}\mathrm{e}^{-\mathrm{i}\hat{H}t/\hbar}] \tag{5.6b}$$

with

$$\hat{F}_r(\beta)e^{-\beta\hat{H}/2}\hat{F}_r e^{-\beta\hat{H}/2} \tag{5.6c}$$

$C_{rr}(t)$ is the flux−flux autocorrelation, as before, for a dividing surface located on the reactant side of the complex region (cf. Figure 8a), and $C_{rp}(t)$ is the cross correlation function between the flux operators $\hat{F}_r$ and $\hat{F}_p$, the latter defined with respect to a dividing surface on the product side of the complex region.

The physical interpretations of eq 5.5 are relatively transparent: reaction can only occur if flux gets from the reactant region r to the product region p without suffering a collision with the bath gas, because in the strong collision approximation a collision with the bath gas relaxes the system and yields recombined product. Since $C_{rp}(t)$ is the probability of flux from region r to region p in time t and $e^{-\omega t}$ is the probability of *not* having a collision with the bath gas in this time interval, eq 5.5b is obtained for the reaction rate. In eq 5.5a, the first term $\int_0^\infty dt\ e^{-\omega t}C_{rr}(t)$, is identified as the total loss rate of reactants, the second term, $\int_0^\infty dt\ e^{-\omega t}C_{rp}(t)$, the loss rate due to reaction, and so their difference, eq 5.5a, is the rate of loss due to recombination. (The collision-free ($\omega \equiv 0$) reaction rate is the time integral of either correlation function, so that the $\omega = 0$ recombination rate is zero.)

Equation 5.5 is seen to have a very useful structure for practical calculation: along the lines described in section IVa, one first finds the eigenvalues and eigenvectors of the Boltzmannized flux operator of eq 5.6c. Each of these eigenvectors is time-evolved, and then the expectation value of either $\hat{F}_r$ or $\hat{F}_p$ is computed with these time-evolved vectors. With the same time evolution one thus obtains both correlation functions in eq 5.6 which are needed to construct the rate constants in eq 5.5.

Figure 10 shows these[48] two correlation functions for reaction 5.4 (for $J = 0$) at $T = 1200$ K. The direct peak is barely discernable in $C_{rr}(t)$ because at this temperature $\hbar\beta \cong 7$ fs $=$ 0.007 ps. The negative lobe of $C_{rr}(t)$, extending to ≅0.5 ps, is due to flux from the $HO_2$ complex that decays back to reactants. The cross correlation function $C_{rp}(t)$ is zero for short times since it takes some time to go from the reactant dividing surface to the product one. The integrals of both of these correlation functions are the same and give the collisionless ($\omega = 0$) reaction rate, but it is readily apparent that it is easier to obtain the $\omega = 0$ reaction rate by computing the integral of $C_{rp}(t)$ rather than $C_{rr}(t)$, so as not to have to deal with the cancellation between the positive short-time direct contribution and the negative long-time recrossing contribution in the latter correlation function. (Metiu et al.[49] have earlier also found it useful for other purposes to use a cross correlation function rather than the autocorrelation function.)

Because of the importance[50] of reaction 5.4 in modeling combustion, it is useful to note some interesting dynamical features of even the zero pressure ($\omega = 0$) bimolecular reaction. If one were to apply ordinary TST, the best choice for the dividing surface would be at $s_r$ in Figure 9b, and then the flux autocorrelation function $C_{rr}(t)$ noted above, and seen in Figure 8b, is the correlation function $C_f(t)$ discussed in section IV. The area under the short-time positive peak of $C_{rr}(t)$ is the incident flux through this surface from the reactant region, and the area under the negative lobe is the part of it that recrosses this dividing surface and goes back to reactants. By computing these areas separately, one finds that ∼69% of the incident flux recrosses the dividing surface; that is, the "transmission coefficient" (the correction factor by which one must multiply the TST rate constant to obtain the correct result) is ≅0.31. This is actually quite surprising, because a *statistical* approximation[51] predicts essentially no recrossing flux for the reaction in the exothermic direction, $O + OH \rightarrow O_2 + H$. The fact that there is so much recrossing flux is presumably due to the inefficient coupling between the O−O motion (the incident reaction coordinate) and the light atom H−$O_2$ motion (the exit reaction coordinate). Interestingly, classical trajectory calculations show[52] approximately this same degree of recrossing flux (i.e., small transmission coefficient).

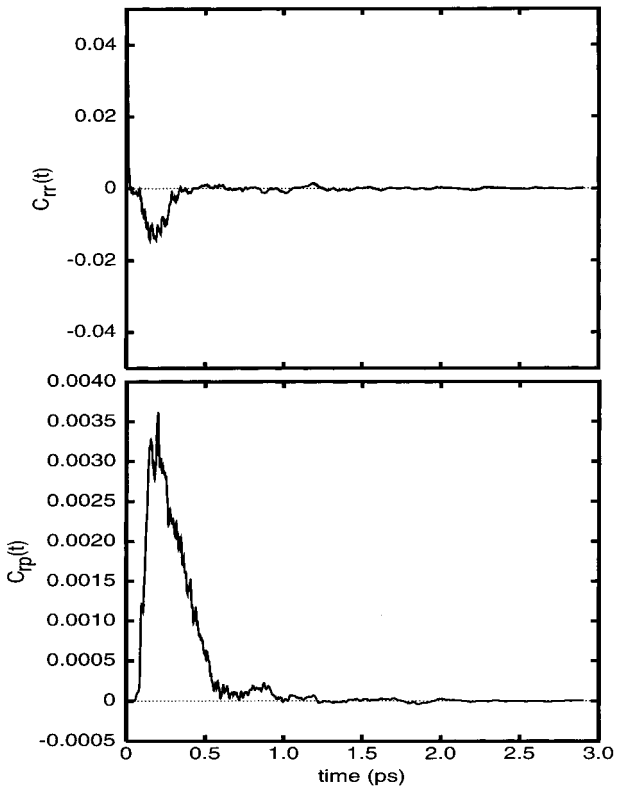


**Figure 10.** Flux−flux correlation functions $C_{rr}(t)$ (top panel) and $C_{rp}(t)$ (bottom panel) for the OH + O → H + $O_2$ reaction at $T = 1200$ °K. Both correlation functions are shown relative to the reactant flux autocorrelation function at zero time, $C_{rr}(0)$.

Finally, Figure 11 shows[48] the pressure dependence of the rate constants for reaction (OH + O → H + $O_2$) and recombination (OH + O → $HO_2$) for a low temperature (500 K, solid lines) and a high temperature (2000 K, dotted lines). (Figures 11a,b are the same results, with a log and linear scale for the abscissa, respectively, to emphasize different regions of pressure.) The reaction rate is essentially independent of pressure until very high pressure (≥100 atm), and up to this same region of pressure the recombination rate has the typical low-pressure limiting form, i.e., linear in the pressure of the bath gas.

## VI. Concluding Remarks

The methodologies described in sections III and IV give one the possibility of carrying out accurate quantum calculations for the rate constants of simple chemical reactions (given, of course, an accurate potential energy surface, which still remains a practical limitation to widespread applications). The microcanonical and canonical versions of the theory are each useful for various applications. For unimolecular reactions (e.g., the ketene isomerization discussed in section III) one is specifically interested in the energy dependence of $k(E)$, while for bimo-

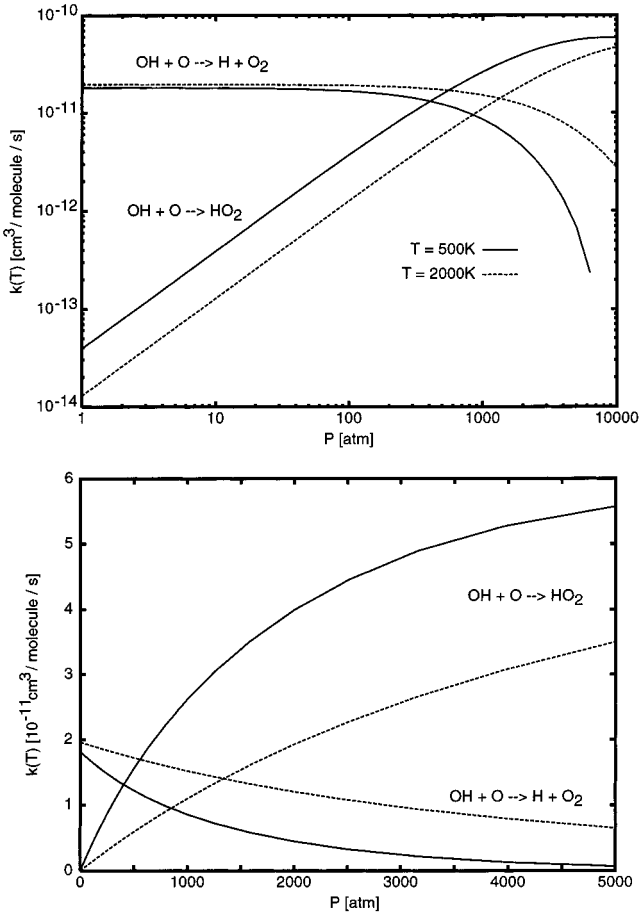


**Figure 11.** Pressure dependence of the reaction and recombination rates for $T = 500$ °K and $T = 2000$ °K. (The upper and lower panels show the same results, with a logarithmic and linear pressure scale, respectively, to emphasize the different regions of pressure.)

lecular reactions one typically wants only $k(T)$ (unless $N(E)$ is desired for interpretational purposes). The microcanonical and canonical approaches focus on the operators $\hat{G}_\epsilon(E)$ and $\exp[-i\hat{H}t/\hbar]$, respectively, but these are essentially the same thing (cf. eq 4.3) and thus entail essentially the same computational effort. Nevertheless the organization of the calculation is often different and more efficient depending on which version of the theory is employed. Methodological advances are thus still taking place.

At best, however, full-blown quantum calculations of the type described above will remain limited to small molecular systems (though "small" may be gradually redefined upward as computer hardware progresses), so that one is always interested in useful approximations that can make the approaches applicable to larger chemical systems. One such approximation of this type was mentioned in section IIb with regard to the ketene isomerization, cf. eqs 3.15, a "reduced dimensionality" approximation of the type advocated by Bowman[31] and his coworkers; the *J*-shifting approximation of section IVc is also of this type. Here one simply assumes that some (perhaps large number of) degrees of freedom are uncoupled from the primary set of degrees of freedom included in the quantum calculation. The uncoupled degrees of freedom are included in the state-counting (which is a convolution structure in the microcanonical case and a multiplicative factor in the canonical case) but not dynamically.

A more accurate way to treat a small primary "system" that is to be described by accurate quantum dynamics, coupled to a secondary "bath" that is treated more approximately, is to include coupling between the two in a *average* manner, e.g., the time-dependent self-consistent-field (TD-SCF) approximation.[53] If one furthermore treats the bath degrees of freedom in the classical limit, then the popular "mixed quantum−classical" Ehrenfest model[54] results, whereby one integrates the time-dependent Schrödinger equation for the quantum degrees of freedom simultaneously with classical equations of motions for the classical degrees of freedom. Metiu et al.[55] have in fact implemented a version of this approach for calculating the flux autocorrelation function, applied to H atom motion on metal surfaces, where the H atom is treated quantum mechanically and the surface motion classically. The methodology of section IVa makes this even more efficient: Wang et al.[56] have recently carried out such a calculation for a (quantum) double-well potential coupled to several hundred (classical) harmonic oscillator (bath) degrees of freedom, obtaining quite reasonable agreement with Topaler and Makri's[57] accurate (fully quantum) path integral simulations for this system. It is also clear that the "bath" in this approach can have a variety of physical manifestations: a liquid solvent, a cluster environment, or a surrounding protein. This thus allows one to combine the rigorous quantum treatments described in this paper for the primary molecular system with classical molecular dynamics simulations of a complex environment.

Other variations on the above theme are possible. One could treat the quantum degrees of freedom above within a *semiclassical* approximation rather than fully quantum mechanically, and this would be the "mixed semiclassical−classical" model recently described by Sun and Miller.[58] Better than this would be to treat *all* the degrees of freedom semiclassically (if this is possible), e.g., the *initial value representation* (IVR)[59] of the semiclassical approximation that is currently receiving a great deal of attention. In the Herman−Kluk[59f] (coherent state) version of the IVR, for example, the time evolution operator is given by an average over the phase space of initial conditions for classical trajectories,

$$e^{-i\hat{H}t/\hbar} = \frac{\int d\mathbf{p}_1 \int d\mathbf{q}_1}{(2\pi\hbar)^F} C_t(\mathbf{p}_1,\mathbf{q}_1) e^{iS_t(\mathbf{p}_1,\mathbf{q}_1)/\hbar} |\mathbf{p}_t,\mathbf{q}_t\rangle\langle\mathbf{p}_1,\mathbf{q}_1| \quad (6.1a)$$

where $|\mathbf{p},\mathbf{q}\rangle$ is a coherent state, i.e., the state whose wave function is a minimum uncertainty (Gaussian) wave packet,

$$\langle\mathbf{x}|\mathbf{p},\mathbf{q}\rangle = \left(\frac{\gamma}{\pi}\right)^{F/4} e^{-(\gamma/2)|\mathbf{x}-\mathbf{q}|^2} e^{(i/\hbar)\mathbf{p}\cdot(\mathbf{x}-\mathbf{q})} \quad (6.1b)$$

$\mathbf{p}_t \equiv \mathbf{p}_t(\mathbf{p}_1,\mathbf{q}_1)$ and $\mathbf{q}_t \equiv \mathbf{q}_t(\mathbf{p}_1,\mathbf{q}_1)$ are the (classically) time-evolved phase space variables, $S_t(\mathbf{p}_1,\mathbf{q}_1)$ is the classical action along the trajectory with these initial conditions, and the preexponential factor $C_t(\mathbf{p}_1,\mathbf{q}_1)$ is the determinant of a particular linear combination of elements of the monodromy matrix,

$$C_t(\mathbf{p}_1,\mathbf{q}_1) = \det\frac{1}{2}\left[\partial\mathbf{q}_t/\partial\mathbf{q}_1 + \partial\mathbf{p}_t/\partial\mathbf{p}_1 - i\hbar\gamma\,\partial\mathbf{q}_t/\partial\mathbf{p}_1 - \frac{1}{i\hbar\gamma}\partial\mathbf{p}_t/\partial\mathbf{q}_1\right] \quad (6.1c)$$

This and other variations of the IVR approach can thus readily be used in the quantum expressions of section III and IV to generate semiclassical approximations for $C_f(t)$ and $N(E)$, and the development of these approaches is a matter of ongoing research. It has also been recently shown[60,61] how this semiclassical IVR approximation can be generalized to include electronic degrees of freedom in a dynamically consistent way with the dynamics of nuclear motion, so that one can use the approach to describe electronically nonadiabatic processes in chemical reactions.

**Acknowledgment.** This work has been supported by the Director, Office of Energy Research, Office of Basic Energy Sciences, Chemical Sciences Division, of the U.S. Department of Energy under Contract No. DE-AC03-76SF00098 and also by the National Science Foundation under Grant No. CHE94-22559.

## References and Notes

(1) See, for example: Miller, W. H. *J. Chem. Phys.* **1969**, *50*, 407.

(2) (a) Miller, W. H.; Jansen op de Haar, B. M. D. D. *J. Chem. Phys.* **1987**, *86*, 6213. (b) Zhang, J. Z. H.; Chu, S. I.; Miller, W. H. *J. Chem. Phys.* **1988**, *88*, 6233. (c) Zhang, J. Z. H.; Miller, W. H. *Chem. Phys. Lett*. **1988**, *153*, 465; **1989**, *159*, 130; *J. Chem. Phys.* **1989**, *91*, 1528. (d) Mielke, S. L.; Truhlar, D. G.; Schwenke, D. W. *J. Chem. Phys.* **1991**, *95*, 5930; *J. Phys. Chem.* **1994**, *98*, 1053.

(3) (a) Kuppermann, A. *J. Phys. Chem.* **1996**, *100*, 2621. (b) Schatz, G. C. *J. Phys. Chem.* **1996**, *100*, 12839. (c) Pack, R. T.; Butcher, E. A.; Parker, G. A. *J. Chem. Phys.* **1995**, *102*, 5998. (d) Castillo, J. F.; Manolopoulos, D. E.; Stark, K.; Werner, H. J. *J. Chem. Phys.* **1996**, *104*, 6531. (e) Launay, J. M.; LeDourneauf, M. *Chem. Phys. Lett*. **1990**, *169*, 473.

(4) Miller, W. H. *J. Chem. Phys.* **1975**, *62*, 1899.

(5) Some reviews of earlier stages of this topic are: (a) Miller, W. H. *Acc. Chem. Res*. **1993**, *26*, 174. (b) Miller, W. H. In *New Trends in Reaction Rate Theory*; Talkner, P., Hänggi, P., Eds.; Kluwer Academic Pub.: Dordrecht, 1995; pp 225−246. (c) Miller, W. H. In *Proceedings of the Robert A. Welch Foundation, 38th Conference on Chemical Research, Chemical Dynamics of Transient Species*; Robert A. Welch Foundation: Houston, TX, 1994; pp 17−27. (d) Miller, W. H. In *Dynamics of Molecules and Chemical Reactions*; Zhang, J., Wyatt, R., Eds.; Marcel Dekker: New York, 1995; pp 387−410. (e) Miller, W. H. *Adv. Chem. Phys.* **1997**, *101*, 853.

(6) Miller, W. H. *J. Chem. Phys.* **1974**, *61*, 1823.

(7) For modern discussions of transition state theory see: (a) Pechukas, P. In *Dynamics of Molecular Collisions*, Part B; Miller, W. H., Ed.; (Vol. 2 of *Modern Theoretical Chemistry*); Plenum: New York, 1976; Chapter 6. (b) Miller, W. H. *Acc. Chem. Res*. **1976**, *9*, 306. (c) Truhlar, D. G.; Hase, W. L.; Hynes, J. T. *J. Phys. Chem.* **1983**, *87*, 2664.

(8) (a) Pechukas, P.; McLafferty, F. J. *J. Chem. Phys.* **1973**, *58*, 1622. (b) Pechukas, P.; McLafferty, F. J. *Chem. Phys. Lett*. **1974**, *27*, 511.

(9) (a) Chapman, S.; Garrett, B. C.; Miller, W. H. *J. Chem. Phys.* **1975**, *63*, 2710. (b) Miller, W. H. *Faraday Discuss. Chem. Soc*. **1977**, *62*, 40. (c) Miller, W. H.; Hernandez, R.; Handy, N. C.; Jayatilaka, D.; Willetts, A. *Chem. Phys. Lett*. **1990**, *172*, 62.

(10) Miller, W. H.; Schwartz, S. D.; Tromp, J. W. *J. Chem. Phys.* **1983**, *79*, 4889.

(11) (a) Yamashita, K.; Miller, W. H. *J. Chem. Phys.* **1985**, *82*, 5475. (b) Thirumalai, D.; Berne, B. J. *J. Chem. Phys.* **1983**, *79*, 5029.

(12) Yamamoto, T. *J. Chem. Phys.* **1960**, *33*, 281.

(13) Kubo, R.; Yokota, M.; Nakajima, S. *J. Phys. Soc. Jpn.* **1957**, *12*, 1203.

(14) Voth, G. A.; Chandler, D.; Miller, W. H. *J. Phys. Chem.* **1989**, *93*, 7009.

(15) Thirumalai, D.; Garrett, B.; Berne, B. J. *J. Chem. Phys.* **1985**, *83*, 2972.

(16) (a) Seideman, T.; Miller, W. H. *J. Chem. Phys.* **1992**, *96*, 4412. (b) Seideman, T.; Miller, W. H. *J. Chem. Phys.* **1992**, *97*, 2499.

(17) (a) Goldberg, A.; Shore, B. W. *J. Phys. B* **1978**, *11*, 3339. (b) Leforestier, C.; Wyatt, R. E. *J. Chem. Phys.* **1983**, *78*, 2334. (c) Kosloff, R.; Kosloff, D. *J. Comput. Phys.* **1986**, *63*, 363. (d) Neuhauser, D.; Baer, M. *J. Chem. Phys.* **1989**, *90*, 4351.

(18) Manthe, U.; Miller, W. H. *J. Chem. Phys.* **1993**, *99*, 3411.

(19) Wu, X. T.; Hayes, E. F. *J. Chem. Phys.* **1997**, *130*, 136.

(20) Zhang, D. H.; Light, J. C. *J. Chem. Phys.* **1996**, *104*, 6184; **1997**, *106*, 551.

(21) Manthe, U. Private communication.

(22) Harris, D. O.; Engerholm, G. G.; Gwinn, W. D. *J. Chem. Phys.* **1965**, *43*, 1515.

(23) (a) Lill, J. V.; Parker, G. A.; Light, J. C. *Chem. Phys. Lett*. **1982**, *89*, 483. (b) Light, J. C.; Hamilton, I. P.; Lill, J. V. *J. Chem. Phys.* **1985**, *82*, 1400. (c) Lill, J. V.; Parker, G. A.; Light, J. C. *J. Chem. Phys.* **1986**, *85*, 900. (d) Bacic, Z.; Light, J. C. *J. Chem. Phys.* **1986**, *85*, 4594. (e) Whitnell, R. M.; Light, J. C. *J. Chem. Phys.* **1988**, *89*, 3674. (f) Choi, S. E.; Light, J. C. *J. Chem. Phys.* **1990**, *92*, 2129.

(24) Colbert, D. T.; Miller, W. H. *J. Chem. Phys.* **1992**, *96*, 1982.

(25) Chatfield, D. C.; Friedman, R. S.; Truhlar, D. G.; Garrett, B. C.; Schwenke, D. W. *J. Am. Chem. Soc.* **1991**, *113*, 486.

(26) (a) Manthe, U.; Seideman, T.; Miller, W. H. *J. Chem. Phys.* **1993**, *99*, 10078. (b) Manthe, U.; Seideman, T.; Miller, W. H. *J. Chem. Phys.* **1994**, *101*, 4759.

(27) Dai, J.; Zhu, W.; Zhang, J. Z. H. *J. Phys. Chem*. **1996**, *100*, 13901.

(28) Zhang, D. H.; Light, J. C. *J. Chem. Phys.* **1996**, *104*, 4544.

(29) Lovejoy, E. R.; Moore, C. B. *J. Chem. Phys.* **1993**, *98*, 7846.

(30) Gezelter, J. D.; Miller, W. H. *J. Chem. Phys.* **1995**, *103*, 7868.

(31) Bowman, J. M. *J. Phys. Chem.* **1991**, *95*, 4960.

(32) Landauer, R. *Philos. Mag*. **1970**, *21*, 863.

(33) Benjamin, I.; Evans, D.; Nitzan, A. *J. Chem. Phys.* **1997**, *106*, 1291.

(34) Vorobeichik, I.; Peskin, U.; Neuhauser, D.; Orenstein, M.; Moiseyev, N. *J. Quant. Elec.* **1997**, *33*, 1236.

(35) Thompson, W. H.; Miller, W. H. *J. Chem. Phys.* **1997**, *106*, 142; Erratum **1997**, *107*, 2164.

(36) (a) Park, T. J.; Light, J. C. *J. Chem. Phys.* **1986**, *85*, 5870. (b) Park, T. J.; Light, J. C. *J. Chem. Phys.* **1988**, *88*, 4897. (c) Park, T. J.; Light, J. C. *J. Chem. Phys.* **1989**, *91*, 974. (d) Park, T. J.; Light, J. C. *J. Chem. Phys.* **1991**, *94*, 2946. (e) Park, T. J.; Light, J. C. *J. Chem. Phys.* **1992**, *96*, 8853. (f) Brown, D.; Light, J. C. *J. Chem. Phys.* **1992**, *97*, 5465.

(37) (a) Manthe, U. *J. Chem. Phys.* **1995**, *102*, 9205. (b) Matzkies, F. Manthe, U. *J. Chem. Phys.* **1997**, *106*, 2646. (c) Matzkies, F.; Manthe, U. *J. Chem. Phys.*, in press.

(38) Wahnström, G.; Metiu, H. *Chem. Phys. Lett*. **1987**, *134*, 531.

(39) Wang, H.; Thompson, W. H.; Miller, W. H. *J. Chem. Phys.* **1997**, *107*, 7194.

(40) McCurdy, C. W.; Miller, W. H. In *State-to-State Chemistry*; Brooks, P. R., Hayes, E. F., Eds.; ACS Symp. Ser. 56; 1977; p 239.

(41) (a) Bowman, J. M. *Chem. Phys. Lett*. **1994**, *217* 36. (b) Qi, J.; Bowman, J. M. *J. Chem. Phys.* **1996**, *105* 9884.

(42) Sun, Q.; Bowman, J. M.; Schatz, G. C.; Sharp, J. R.; Connor, J. N. L. *J. Chem. Phys.* **1990**, *92*, 1677.

(43) For example, Gilbert, R. G.; Smith, S. C. In *Theory of Unimolecular and Recombination Reactions*; Blackwell: Oxford, 1990.

(44) Miller, W. H. *J. Phys. Chem.* **1995**, *99*, 12387.

(45) Miller, W. H. *Faraday Discuss*. **1995**, *102*, 53.

(46) Qi, J.; Bowman, J. M. *J. Phys. Chem.* **1996**, *100*, 15165.

(47) Mandelshtam, V. A.; Taylor, H. S.; Miller, W. H. *J. Chem. Phys.* **1996**, *105*, 496.

(48) Germann, T. C.; Miller, W. H. *J. Phys. Chem*. **1997**, *101*, 6358.

(49) Wahnström, G.; Haug, K.; Metiu, H. *Chem. Phys. Lett*. **1988**, *148*, 158; *J. Chem. Phys.* **1989**, *90*, 540.

(50) Miller, J. A.; Kee, R. J.; Westbrook, C. K. *Annu. Rev. Phys. Chem*. **1990**, *41*, 345.

(51) Duchovic, R. J.; Pettigrew, J. D.; Welling, B.; Shipchandler, T. *J. Chem. Phys.* **1996**, *105*, 10367.

(52) Miller, J. A.; Garrett, B. C. *Int. J. Chem. Kinet*. **1997**, *29*, 275.

(53) See for example: Gerber, R. B.; Buch, V.; Ratner, M. A. *J. Chem. Phys.* **1982**, *77*, 3022.

(54) See, for example: Billing, G. D. *Chem. Phys. Lett*. **1975**, *30*, 391; *J. Chem. Phys.* **1976**, *64*, 908.

(55) Wahnström, G.; Carmeli, B.; Metiu, H. *J. Chem. Phys.* **1988**, *88*, 2478.

(56) Wang, H.; Sun, S.; Miller, W. H. *Chem. Phys. Lett*., in press.

(57) Topaler, M.; Makri, N. *J. Chem. Phys.* **1994**, *101*, 7500.

(58) Sun, X.; Miller, W. H. *J. Chem. Phys.* **1997**, *106*, 916.

(59) (a) Miller, W. H. *J. Chem. Phys.* **1970**, *53*, 3578. (b) Heller, E. J. *J. Chem. Phys.* **1991**, *94*, 2723. (c) Miller, W. H. *J. Chem. Phys.* **1991**, *95*, 9428. (d) Heller, E. J. *J. Chem. Phys.* **1991**, *95*, 9431. (e) Kay, K. G. *J. Chem. Phys.* **1997**, *107*, 2313. (f) Herman, M. F.; Kluk, E. *Chem. Phys*. **1984**, *91*, 27. (g) Campolieti, G.; Brumer, P. *J. Chem. Phys.* **1992**, *96*, 5969.

(60) Sun, X.; Miller, W. H. *J. Chem. Phys.* **1997**, *106*, 6346.

(61) Stock, G.; Thoss, M. *Phys. Rev. Lett.* **1997**, *78*, 578.